J Korean Soc Appl Biol Chem (2015) 58(4):617–625
DOI 10.1007/s13765-015-0076-0

Online ISSN 2234-344X
Print ISSN 1738-2203

ARTICLE

Hepatoprotective effect of phenylethanoid glycosides from *Incarvillea compacta* against CCl_4-induced cytotoxicity in HepG2 cells

Ting Shen[1,2] · Xueqin Li[3] · Weicheng Hu[2] · Lijin Zhang[1] · Xudong Xu[1] · Haifeng Wu[1] · Lilian Ji[2]

Received: 26 February 2015 / Accepted: 21 April 2015 / Published online: 30 May 2015

Abstract The extraction and solvent partition of roots of *Incarvillea compacta*, a traditional Tibetan folk medicine, and repeated column chromatography and preparative high-performance liquid chromatography for *n*-butanol fraction yielded four phenylethanoid glycosides, crenatoside (**1**), 3‴-*O*-methylcrenatoside (**2**), leucoseceptoside A (**3**), and martynoside (**4**). The chemical structures were identified on the basis of spectroscopic data analyses including NMR and MS. All compounds were isolated for the first time from the plant. Compound **1** exerted better 1,1-diphenyl-2-picrylhydrazyl free radical scavenging activity. In addition, compounds **1**–**4** were evaluated for their hepatoprotective activity on carbon tetrachloride (CCl_4)-induced liver injury in HepG2 cells. Pretreatment of HepG2 cells with compound **1**–**4** significantly increased the viability on CCl_4-induced cell death. Furthermore, compounds **1**–**4** also alleviated CCl_4-induced hepatotoxicity by enhancement of the antioxidant enzyme activities of superoxide dismutase and reduction of the malondialdehyde content, intracellular ROS as well as NF-κB transactivation. Our results suggest that phenylethanoid glycosides ameliorate CCl_4-induced cell injury, and this protection was likely due to antioxidative activity and down-regulation of NF-κB.

Keywords Hepatoprotective activity · *Incarvillea compacta* · Phenylethanoid glycoside · Reactive oxygen species

Ting Shen and Xueqin Li contributed equally to this work.

Electronic supplementary material The online version of this article (doi:10.1007/s13765-015-0076-0) contains supplementary material, which is available to authorized users.

✉ Haifeng Wu
hfwu@implad.ac.cn

✉ Lilian Ji
jll2663@sina.com

[1] Key Laboratory of Bioactive Substances and Resources Utilization of Chinese Herbal Medicine, Ministry of Education, Institute of Medicinal Plant Development, Peking Union Medical College and Chinese Academy of Medical Sciences, Beijing 100193, China

[2] Jiangsu Collaborative Innovation Center of Regional Modern Agriculture & Environmental Protection/Jiangsu Key Laboratory for Eco-Agricultural Biotechnology Around Hongze Lake, Huaiyin Normal University, Huaian 223300, China

[3] Department of Gerontology, Huai'an First People's Hospital, Nanjing Medical University, 6 Beijing West Road, Huaian 223300, China

Introduction

Hepatic disease is a major worldwide health problem with high endemicity in developing countries mainly caused by infection, chemicals, and excessive drug therapy (Adewusi and Afolayan 2010). Despite advances in modern medicine, there is lack of effective drug to stimulate liver function, offer protection to the liver from damage, or help regenerate hepatic cells (Chattopadhyay 2003). Thus, it is imperative to search for new drugs for the treatment of liver disorders. Undoubtedly, herbal therapy offers effectual alternatives to the limited therapeutic options considering that many herbal medicines have been clinically used as hepatoprotective agents, such as silymarin, andrographolide, and glycyrrhizin (Kashaw et al. 2011). CCl4-induced damage is able to change the antioxidant status of the tissues including swelling, necrosis of hepatocytes, and the release of cytosolic enzymes, such as glutamic

oxaloacetic transaminase (GOT), glutamic pyruvic transaminase (GPT), alkaline phosphatase (ALP), and lactate dehydrogenase (LDH) into serum and eventually kills cells (Dai et al. 2014; Yu et al. 2011). Therefore, antioxidative property is claimed to be one of the mechanisms of hepatoprotective effect (Bhardwaj et al. 2011).

Incarvillea compacta Maxim (Bignoniaceae) is a perennial herb mainly native to the mountains of Qinghai, Tibetan, and Yunnan provinces of China (Delectis Florae Reipublicae Popularis Sinicae Agendae Academiae Sinicae Edita 1990) and is traditionally used as Tibetan folk medicine for the treatment of jaundice, dyspepsia, and gastralgia (Yang 1991). In spite of the popular use, there is so far no report about chemical composition of the plant. Previous investigations on the genus *Incarvillea* have led to the isolation of monoterpenoid alkaloids (Chi et al. 2005; Fu et al. 2007), iridoids (Lu et al. 2007), and sesquiterpenes (Fu et al. 2010; Yan et al. 2012). Several studies on antinociceptive effect were also carried out (Nakamura et al. 1999, 2001). Although clinical documentation is scare as far as hepatoprotective activity is concerned, some local traditional practitioners have reported favorable results with powdered extract of the plant. Thus, the present study was initiated to search for hepatoprotective constituents from *I. compacta*, and four phenylethanoid glycosides were finally isolated. Phenylethanoid glycosides reportedly display a variety of pharmacological activities including antioxidative, anti-inflammatory, and hepatoprotective activities (Fu et al. 2008). Therefore, the isolated phenylethanoid glycosides from *I. compacta* were evaluated for antioxidative and hepatoprotective effects using HepG2 cells. Herein, we describe the isolation of four phenylethanoid glycosides, and their antioxidative and hepatoprotective effects.

Materials and methods

Plant material

Incarvillea compacta roots were collected in Huzhu County, China in July 2013, and identified by Prof. Xiao-Feng Zhang of the Department of Tibetan medicines, Northwest Institute of Plateau Biology, Chinese Academy of Sciences. A voucher specimen (No. 130718) was deposited at the Key Laboratory of Bioactive Substances and Resource Utilization of Chinese Herbal Medicine, Ministry of Education, Institute of Medicinal Plant Development, Peking Union Medical College, and Chinese Academy of Medical Sciences.

General experimental procedures

NMR spectra were obtained with a Bruker AV III 600 NMR spectrometer (chemical shift values are presented as δ values with TMS as the internal standard). ESIMS spectra were performed on a LTQ-Obitrap XL spectrometer. Preparative high-performance liquid chromatography (HPLC) was performed on a Lumtech K1001 analytic LC equipped with two pumps of K-501, a UV detector of K-2600, and an YMC semi-preparative column (250 mm × 10 mm) packed with C_{18} (5 μm). C_{18} reversed-phase silica gel (40–63 μm, Merk, Germany), Sephadex LH-20 (Pharmacia, Sweden), and silica gel (100–200 and 300–400 mesh, Qingdao Marine Chemical plant, People's Republic of China) were used for column chromatography. Precoated silica gel GF_{254} plates (Zhi Fu Huang Wu Pilot Plant of Silica Gel Development, Yantai, People's Republic of China) were used for TLC. All solvents used were of analytical grade (Beijing Chemical Works). 1,1-diphenyl-2-picrylhydrazyl (DPPH) and 3-(4,5-dimethylthiazol-2-yl)-2,5- diphenyltetrazolium bromide (MTT) were purchased from Sigma (USA). Dulbecco's modified Eagle medium (DMEM) medium and antibiotics were acquired from Gibco BRL (Life Technologies, China). Fetal bovine serum (FBS) was obtained from Gibco BRL (USA). The culture supplies were obtained from Corning (USA).

Extraction, fractionation, and isolation

The air-dried and powdered roots of *I. compacta* (1.2 kg) were extracted three times with 90 % ethanol (3 × 3 L) at room temperature. Removal of the ethanol under reduced pressure yielded the extract (98 g). The extract was suspended in distilled water (1 L) and then the suspension was partitioned with ethyl acetate and *n*-BuOH, successively, yielding the EtOAc fraction (18 g), the *n*-BuOH fraction (37 g), and the H_2O fraction (32 g). The *n*-BuOH soluble fraction (37 g) was subjected to silica gel (100–200 mesh) column chromatography using a $CHCl_3$–MeOH gradient (from 50:1 to 0:1) as eluent, to yield five fractions (Fr. A–G). Fr. C (4.8 g) was applied to C_{18} reversed-phase silica gel and Sephadex LH-20 column to afford five fractions (Fr. C1–C5). Fr. C3 (590 mg) was subjected to semi-preparative liquid chromatography using an MeOH–H_2O (43:57) system to yield **1** (11.9 mg) and **2** (15.2 mg). Fr. D (5.1 g) was subjected to C_{18} reversed-phase silica gel and four fractions (Fr. D1–D4) were collected. Fr. D2 (650 mg) was separated by semi-preparative liquid chromatography using an MeOH–H_2O (46:54) system to yield **3** (22.7 mg) and **4** (12.3 mg).

*Compound **1***

White amorphous powder; positive ESI–MS *m/z* 645 $[M+Na]^+$, 1267 $[2M+Na]^+$; ^1H NMR (600 MHz, CD_3OD, δ_H) 6.83 (1H, br s, H-2), 6.73 (1H, d, $J = 7.8$ Hz,

H-5), 6.68 (1H, br d, $J = 7.2$ Hz, H-6), 4.60 (1H, dd, $J = 10.0$, 1.8 Hz, H-7), 3.98 (1H, dd, $J = 12.0$, 1.8 Hz, H-8α), 3.61 (1H, m, H-8β), 4.54 (1H, d, $J = 7.8$ Hz, H-1′), 3.45 (1H, m, H-2′), 4.13 (1H, t, $J = 9.6$ Hz, H-3′), 5.10 (1H, t, $J = 9.6$ Hz, H-4′) 3.78 (1H, m, H-5′), 3.66 (1H, m, H-6′α), 3.59 (1H, m, H-6′β), 5.17 (1H, brs, H-1″), 3.78 (1H,br s, H-2″), 3.53 (1H, m, H-3″), 3.27 (1H, t, $J = 9.6$ Hz, H-4″), 3.78 (1H, m, H-5″), 1.12 (3H, d, $J = 6.0$ Hz, H-6″), 7.07 (1H, br s, H-2‴), 6.78 (1H, d, $J = 7.8$ Hz, H-5‴), 6.96 (1H, br d, $J = 7.8$ Hz, H-6‴), 7.60 (1H, d, $J = 16.2$ Hz, H-7‴), 6.27 (1H, d, $J = 16.2$ Hz, H-8‴); ^{13}C NMR (150 MHz, CD_3OD, δ_C) 130.0 (C-1), 114.7 (C-2), 146.6 (C-3), 146.6 (C-4), 116.5 (C-5), 119.2 (C-6), 78.7 (C-7), 73.2 (C-8), 99.3 (C-1′), 82.2 (C-2′), 77.4 (C-3′), 70.5 (C-4′), 78.1 (C-5′), 62.3 (C-6′), 102.4 (C-1″), 72.2 (C-2″), 72.3 (C-3″), 73.8 (C-4″), 70.5 (C-5″), 18.3 (C-6″), 127.8 (C-1‴), 114.5 (C-2‴), 147.1 (C-3‴), 150.2 (C-4‴), 116.7 (C-5‴), 123.6 (C-6‴), 148.4 (C-7‴), 115.4 (C-8‴), 168.2 (C-9‴).

Compound ***2***

White amorphous powder; positive ESI–MS *m/z* 659 $[M+Na]^+$, 1295 $[2M+Na]^+$; ^{1}H NMR (600 MHz, CD_3OD, δ_H) 6.83 (1H, br s, H-2), 6.72 (1H, d, $J = 8.4$ Hz, H-5), 6.69 (1H, br d, $J = 7.8$ Hz, H-6), 4.60 (1H, dd, $J = 10.0$, 1.8 Hz, H-7), 3.98 (1H, dd, $J = 12.0$, 1.8 Hz, H-8α), 3.61 (1H, m, H-8β), 4.55 (1H, d, $J = 7.8$ Hz, H-1′), 3.45 (1H, m, H-2′), 4.13 (1H, t, $J = 9.6$ Hz, H-3′), 5.10 (1H, t, $J = 9.6$ Hz, H-4′), 3.78 (1H, m, H-5′), 3.66 (1H, m, H-6′α), 3.59 (1H, m, H-6′β), 5.19 (1H brs, H-1″), 3.78 (1H, br s, H-2″), 3.53 (1H, m, H-3″), 3.27 (1H, t, $J = 9.6$ Hz, H-4″), 3.78 (1H, m, H-5″), 1.12 (3H, d, $J = 6.0$ Hz, H-6″), 7.21 (1H, br s, H-2‴), 6.81 (1H, d, $J = 7.8$ Hz, H-5‴), 7.09 (1H, br s, $J = 8.4$ Hz, H-6‴), 7.67 (1H, d, $J = 16.2$ Hz, H-7‴), 6.37 (1H, d, $J = 16.2$ Hz, H-8‴), 3.90 (3H, s, 3‴-OCH_3); ^{13}C NMR (150 MHz, CD_3OD, δ_C) 130.0 (C-1), 114.7 (C-2), 146.6 (C-3), 146.6 (C-4), 116.5 (C-5), 119.1 (C-6), 78.7 (C-7), 73.2 (C-8), 99.3 (C-1′), 82.2 (C-2′), 77.4 (C-3′), 70.5 (C-4′), 78.1 (C-5′), 62.4 (C-6′), 102.4 (C-1″), 72.2 (C-2″), 72.3 (C-3″), 73.8 (C-4″), 70.5 (C-5″), 18.3 (C-6″), 127.9 (C-1‴), 112.1 (C-2‴), 149.6 (C-3‴), 151.1 (C-4‴), 116.7 (C-5‴), 124.6 (C-6‴), 148.3 (C-7‴), 115.1 (C-8‴), 168.2 (C-9‴), 56.7 (3‴-OCH_3).

Compound ***3***

Pale yellow amorphous powder; positive ESI–MS *m/z* 661 $[M+Na]^+$, 1299 $[2M+Na]^+$; ^{1}H NMR (600 MHz, CD_3OD, δ_H) 6.73 (1H, d, $J = 2.4$ Hz, H-2), 6.82 (1H, d, $J = 8.4$ Hz, H-5), 6.57 (1H, dd, $J = 8.4$, 2.4 Hz, H-6), 2.77 (2H, m, H-7), 4.07 (1H, m, H-8α), 3.81 (1H, m, H-8β), 4.38 (1H, d, $J = 8.4$ Hz, H-1′), 3.45 (1H, m, H-2′), 4.13 (1H, t, $J = 9.6$ Hz, H-3′), 4.99 (1H, t, $J = 9.6$ Hz, H-4′), 3.78 (1H, m, H-5′), 3.66 (1H, m, H-6′α), 3.59 (1H, m, H-6′β), 5.20 (1H, br s, H-1″), 3.78 (1H, br s, H-2″), 3.53 (1H, m, H-3″), 3.27 (1H, t, $J = 9.6$ Hz, H-4″), 3.78 (1H, m, H-5″), 1.10 (3H, d, $J = 6.0$ Hz, H-6″), 7.20 (1H, d, $J = 1.8$ Hz, H-2‴), 6.81 (1H, d, $J = 8.4$ Hz, H-5‴), 7.08 (1H, dd, $J = 8.4$, 1.8 Hz, H-6‴), 7.65 (1H, d, $J = 15.6$ Hz, H-7‴), 6.36 (1H, d, $J = 16.2$ Hz, H-8‴), 3.89 (3H, s, 3‴-OMe); ^{13}C NMR (150 MHz, CD_3OD, δ_C) 131.6 (C-1), 116.3 (C-2), 144.8 (C-3), 146.2 (C-4), 117.3 (C-5), 121.4 (C-6), 36.7 (C-7), 72.3 (C-8), 104.3 (C-1′), 76.3 (C-2′), 81.7 (C-3′), 70.6 (C-4′), 76.4 (C-5′), 62.5 (C-6′), 102.6 (C-1″), 72.3 (C-2″), 72.6 (C-3″). 74.0 (C-4″), 70.9 (C-5″), 18.4 (C-6″), 127.8 (C-1‴), 111.9 (C-2‴), 150.9 (C-3‴), 149.5 (C-4‴), 116.7 (C-5‴), 124.6 (C-6‴), 148.1 (C-7‴), 115.3 (C-8‴), 168.4 (C-9‴), 56.6 (3‴-OMe).

Compound ***4***

Pale yellow amorphous powder; positive ESI–MS *m/z* 675 $[M+Na]^+$, 691 $[M+K]^+$, 1327 $[2M+Na]^+$;^{1}H NMR (600 MHz, CD_3OD, δ_H) 6.73 (1H, d, $J = 2.4$ Hz, H-2), 6.82 (1H, d, $J = 8.4$ Hz, H-5), 6.68 (1H, dd, $J = 8.4$, 2.4 Hz, H-6), 2.82 (2H, m, H-7), 4.07 (1H, m, H-8α), 3.81 (1H, m, H-8β), 4.38 (1H, d, $J = 7.8$ Hz, H-1′), 3.45 (1H, m, H-2′), 4.13 (1H, t, $J = 9.6$ Hz, H-3′), 4.99 (1H, t, $J = 9.6$ Hz, H-4′), 3.78 (1H, m, H-5′), 3.66 (1H, m, H-6′), 3.59 (1H, m, H-6′), 5.20 (1H, d, $J = 1.8$ Hz, H-1″), 3.78 (1H, br s, H-2″), 3.53 (1H, m, H-3″), 3.27 (1H, t, $J = 9.6$ Hz, H-4″), 3.78 (1H, m, H-5″), 1.11 (3H, d, $J = 6.0$ Hz, H-6″), 7.20 (1H, d, $J = 1.8$ Hz, H-2‴), 6.81 (1H, d, $J = 8.4$ Hz, H-5‴), 7.08 (1H, dd, $J = 8.4$, 1.8 Hz, H-6‴), 7.65 (1H, d, $J = 16.2$ Hz, H-7‴), 6.36 (1H, d, $J = 16.2$ Hz, H-8‴), 3.89 (3H, s, 3‴-OCH_3), 3.82 (3H, s, 4-OCH_3); ^{13}C NMR (150 MHz, CD_3OD, δ_C) 133.2 (C-1). 113.1 (C-2), 147.6 (C-3), 147.8 (C-4), 117.3 (C-5), 121.4 (C-6), 36.7 (C-7), 72.3 (C-8), 104.4 (C-1′) 76.3 (C-2′), 81.7 (C-3′), 70.6 (C-4′), 76.4 (C-5′), 62.6 (C-6′), 103.2 (C-1″), 72.3 (C-2″), 72.6 (C-3″), 74.0 (C-4″), 70.9 (C-5″), 18.4 (C-6″), 127.8 (C-1‴), 112.1 (C-2‴), 151.1 (C-3‴), 149.6 (C-4‴), 116.7 (C-5‴), 124.6 (C-6‴), 148.1 (C-7‴), 115.3 (C-8‴), 168.5 (C-9‴), 56.7 (4-OCH_3), 56.6 (3‴-OCH_3).

DPPH free radical scavenging activity

The DPPH free radical scavenging capacity was estimated according to the previously reported procedure (Yang and Lee 2012). Briefly, 100 μL of 0.4 mM DPPH (in methanol) was added to a 96-well plate containing same volume of diluted sample at various concentrations. The mixtures were shaken vigorously and left to stand in the dark at room temperature for 30 min. The decrease in absorbance at 517 nm was measured using an Infinite M200 Pro

spectrophotometer (Tecan, Switzerland). The data were recorded using the software package Magellan 6.3.

DPPH radical scavenging activity was calculated using the following equation:

$$\text{Scavenging effect}\,(\%) = [1 - (A_i - A_j)/A_0] \times 100,$$

where A_0 is the A_{517} of DPPH without sample (control), A_i is the A_{517} of sample and DPPH, and A_j is the A_{517} of sample without DPPH (blank). The effective concentration required for 50 % plaque reduction (IC_{50}) was determined from a curve relating plaque number to the concentration of a sample. All tests were run in triplicate, and the average value was calculated.

HepG2 cell culture

Human HepG2 hepatoma cells were purchased from the Cell Bank of Chinese Academy of Sciences (Shanghai, China). HepG2 cells were grown in DMEM medium supplemented with 10 % FBS, 100 μg/mL penicillin, and 100 μg/mL streptomycin. Cells were incubated at 37 °C in a moist atmosphere containing 5 % CO_2.

Hepatoprotective activity assay

HepG2 cells (5×10^4/well) were plated in a 96-well plate for 16 h. Then, the medium was aspirated and replaced with serum-free medium of different samples for 6 h. After removing the supernatant of each well, a total of 10 μL of MTT solution was added to each well at the time of incubation for 4 h. The formazan crystals were solubilized with 100 μL of MTT stop solution and measured using an Infinite M200 Pro spectrophotometer (Hu et al. 2014). Cytoprotective activity of test samples on CCl_4-induced cell injury was investigated. In total, 5×10^4 cells were plated per well in 96-well plates with culture medium for 16 h and then exposed to test samples for 30 min before exposure to 0.4 % CCl_4 for 6 h. Cell viability was determined as described above and the percentage cell viability was expressed as a percentage with the control cells treated with vehicle as 100 %. Following treatment, the cells were harvested and resuspended in 0.4 % trypan blue solution. The number of blue-stained (dead) and unstained (viable) cells were counted using a hemocytometer.

Intracellular ROS inhibition activity

5×10^4 cells were plated per well in 96-well plates with culture medium for 16 h and then exposed to test samples for 30 min before exposure to 0.4 % CCl_4 for 6 h. After treatment, the supernatant of each well was removed and cells were washed twice with PBS; then DCFH-DA (10 μM) was added and the cells were incubated for 20 min. DCFH-DA was removed from each well and 100 μL cold PBS was added; ROS level was measured using an Infinite M200 Pro spectrophotometer (Tecan, Switzerland) with the excitation wavelength at 488 nm and emission wavelength at 535 nm, respectively.

Measurement of malondialdehyde (MDA) content and SOD activity

A total of 1×10^6 cells was plated per well in 6-well plates for 16 h and then exposed to test samples for 30 min before exposure to 0.4 % CCl_4 for 6 h. Cells were washed twice with PBS, suspended in 0.4 mL of PBS, and sonicated for 20 s. The homogenate was then centrifuged at $6000 \times g$ for 10 min, and the supernatant was collected for further experiments. The MDA content was determined by the thiobarbituric acid reactive substances (TBARS) assay. Homogenate superoxide dismutase (SOD) activity was determined using commercial colorimetric SOD assay kit from Cayman Chemical Company (Ann Arbor, MI).

Luciferase reporter gene activity assay

The HepG2 cells (5×10^5 cells/mL) were transfected with 0.4 μg of plasmids containing NF-κB (Stratagene, USA) as well as β-galactosidase, using the Lipofectamine 2000 (Invitrogen, USA) in the 12-well plates. After 24 h, the transfected cells were treated with test samples in the presence or absence of PMA. Luciferase assays were performed using the luciferase assay system (Promega, USA).

Nuclear protein extraction and Western blot

A total of 5×10^6 cells was plated per well in 6-well plates for 16 h and then exposed to test samples for 30 min before exposure to 0.4 % CCl_4 for 6 h. After washed twice with PBS, the nuclear protein was extracted using nuclear protein isolation kit (ComWin Biotech, China). Aliquots of the lysates (20 μg of protein) were boiled at 95 °C for 5 min and separated on a sodium dodecyl sulfate–polyacrylamide gel and transferred to polyvinylidene difluoride (PVDF; Bio-Rad, USA) membranes. Bound antibodies were detected by ECL system (Thermo Fisher, USA) and blots were observed with the Tanon 5200 chemiluminescence detection (Tanon Science, China).

Statistical analysis

Data are expressed as the mean ± standard derivation (SD). One-way analysis of variance (ANOVA) was used to determine the significant differences between the groups. Values were considered to be significant when $p < 0.05$.

All analyses were performed using SPSS for Windows 7 version 19.0 (SPSS Inc., USA).

Results and discussion

Elucidation of chemical structures of isolated compounds

The roots of *I. compacta* were extracted in 90 % EtOH, and concentrated extracts were successively partitioned into EtOAc, *n*-BuOH, and H_2O fractions. Repeated column chromatography for the *n*-BuOH fraction using SiO_2, ODS resins, Sephadex LH-20, and preparative HPLC yielded four phenylethanoid glycosides (Fig. 1). The chemical structure of the compounds was determined on the basis of spectroscopic analysis, such as NMR and MS.

Compound **1** was obtained as a white amorphous powder and gave a gray–green coloration characteristic of catechol with 1 % ethanolic $FeCl_3$ solution on TLC. The positive-ion ESIMS gave pseudo-molecular ion peaks $[M+Na]^+$ and $[2M+Na]^+$ at *m/z* 645 and 1267, respectively, consistent with the molecular formula $C_{29}H_{34}O_{15}$. The ^{1}H NMR spectrum of compound **1** exhibited characteristic signals arising from (*E*)-caffeoyl acid and 3,4-dihydroxy-phenylethanol moieties: six aromatic proton signals (2 × ABX systems, in the region of δ_H 6.68–7.07), two *trans*-olefinic proton signals (AB system, δ_H 7.60, d, J_{AB} = 16.2 Hz and 6.27, d, J_{AB} = 16.2 Hz), and oxygenated methylene (δ_H 4.60, 1H, dd, J = 10.0, 1.8 Hz) proton signals together with two non-equivalent proton signals (δ_H 3.98, dd, J = 12.0, 1.8 Hz and δ_H 3.61, m) attributed to the side chain of the phenethyl alcohol moiety, two anomeric protons of β-glucose at δ_H 4.54 (1H, d, J = 7.8 Hz), and α-rhamnose at δ_H 5.17 (1H, br s). The above assignments were confirmed by the ^{13}C NMR spectrum, which showed 29 carbon resonance signals. Compound **1** was identified to be crenatoside and confirmed by comparison with those of the literature (Afifi et al. 1993). The NMR spectrum data of compound **2** were very similar to that of **1** with the exception of an extra methoxy group at δ_H 3.90 (3H, s), which was assigned as 3‴-*O*-methylcrenatoside (Li et al. 2004). The ^{1}H and ^{13}C NMR spectra of compounds **3** and **4** were similar and resembled those of **2**. The only difference is that 3,4-dihydroxy-phenylethanol moiety in **3** was replaced by 3-hydroxy-4-methoxyphenylethanol part in **4**. Compounds **3** and **4** were identified as leucoseceptoside A and martynoside (Lu et al. 2009), respectively.

Antiradical activity

DPPH is a stable free radical with a characteristic absorption at 517 nm that decreases significantly on exposure to proton radical scavengers. It has bee extensively used to evaluate the antioxidative ability because it is stabilized and simple (Gulçin et al. 2012). The assay was conducted in methanol, and the results are expressed as IC_{50}, which represent the concentration of a sample scavenging 50 % of the DPPH free radicals in a given experimental situation (Fig. 2). Based on the calculated IC_{50} values, the order of activity was as follows: compound **1** (24.76 μM) > compound **2** (27.82 μM) > compound **3** (53.32 μM) > compound **4** (81.59 μM). Furthermore, result showed that DPPH free radical scavenging activity of compounds **1**–**4** was relatively more pronounced than that of BHT, but weaker than that of L-ascorbic acid (data not shown). Antioxidative property of phenylethanoid glycosides may be due to the number of phenolic hydroxyl groups, steric hindrance, the location of phenolic hydroxyl, and α, β-unsaturated ketone of phenyl-2-propenoyl (Yang et al. 2009).

Effect of isolated compounds on viability of CCl_4-induced HepG2 cells

HepG2 cell line has been proposed as a good model to study in vitro toxicity to the liver since it retains many of the specialized functions (Akanitapichat et al. 2010; Balasubramaniyan et al. 2007). We first studied the response of HepG2 cells to CCl_4 dose by MTT assay and flow cytometry. The cell viability ratio of the control group

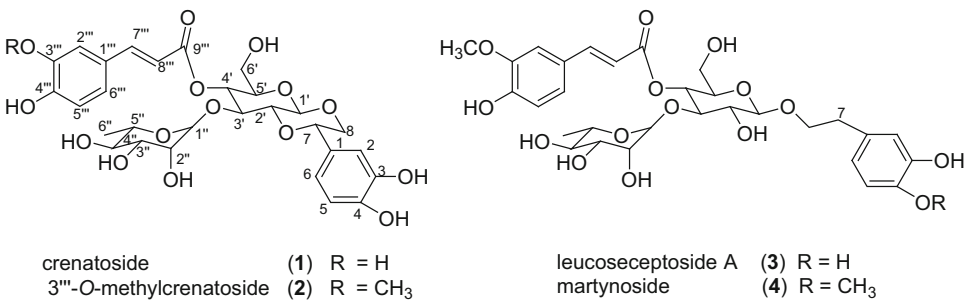

Fig. 1 Chemical structures of compounds **1**–**4** from the roots of *I. compacta*

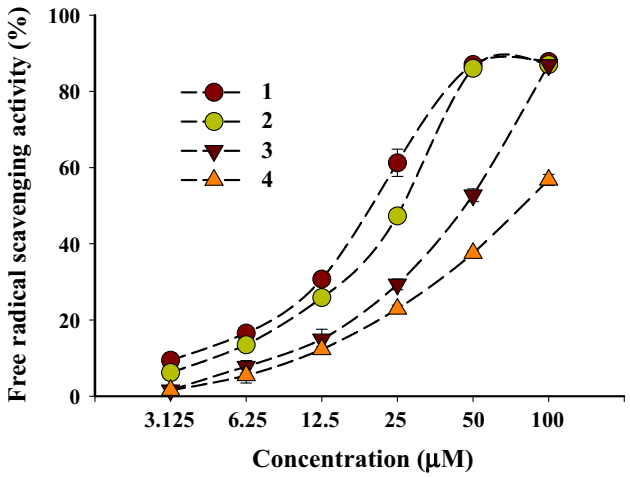

Fig. 2 DPPH free radical scavenging activity of compounds **1–4** obtained from *I. compacta*. Each value is expressed as the mean ± SD ($n = 3$)

was regarded as 100 %. Result had revealed that CCl_4 ranging from 0.1 to 1 % leads to cell death in a dose-dependent manner and 0.4 % CCl_4 mildly affected cell viability (data not shown). In the subsequent studies, cell incubation was conducted with 0.4 % of CCl_4 for 6 h to induce 40–50 % of cell death. As shown in Fig. 3A, B, there was no apparent cytotoxic or inhibitory effect on the growth of HepG2 cells with compounds **1–4** at 0.5 mM based on MTT and trypan blue exclusion experiments. As illustrated in Fig. 3C, D, treatment with 0.4 % of CCl_4 alone resulted in cell death, suggesting that HepG2 cells were very sensitive to CCl_4. However, pretreatment with compounds **1–4** protected cells from CCl_4-induced damage, restoring cell survival. At 100 μM, compounds **1–3** showed the similar hepatoprotective effect, and compound **4** showed weaker efficacy. Moreover, the potency of 100 μM quercetin was similar to that of 100 μM compounds **1–3** (data not shown). Results suggested that the protective effect of compounds isolated from *I. compacta* was not attributable to an effect on the cell division.

Effect of compounds 1–4 on lipid peroxidation in CCl_4-induced HepG2 cells

CCl_4-induced toxicity in human hepatoma HepG2 cell line can be caused by a direct solvent effect or by generation of free radicals and subsequent initiation of lipid peroxidation. Lipid peroxidation, which involves the oxidative alteration of polyunsaturated fatty acids in cell membranes, generates several types of free radicals. The lipid radical is rapidly quenched by molecular oxygen to create a peroxyl-fatty acid radical, which can generate end products such as MDA and unsaturated aldehydes (Lobo et al. 2010; Barrera 2012). To investigate the consequences of CCl_4-induced oxidative damage to cellular macromolecules and to explore the possible protective effects of compounds **1–4**, we determined the formation of MDA. As shown in Fig. 3E, the level of MDA increased significantly to 206.78 % compared to the negative control upon treatment with CCl_4. In contrast, pretreatments with compounds **1–4** inhibited CCl_4-induced lipid peroxidation in HepG2 cells to 156.46, 158.43, 177.73, and 186.54 %, respectively. These results suggest that compounds **1–4** have the potential to suppress intracellular MDA formation induced by CCl_4, and compounds **1** and **2** exerted a stronger cytoprotective effect.

Effect of compounds 1–4 on intracellular ROS production in CCl_4-induced HepG2 cells

The effects of the compounds **1–4** on intracellular ROS generation induced by CCl_4 were estimated using cell-permeable ROS-sensitive fluorophore DCF-DA. CCl_4 treatment for 6 h caused an increase in fluorescence (267.52 % of untreated group), indicating that CCl_4 is capable of inducing ROS formation in HepG2 cells as compared to the control cells (Fig. 4A). Incubation of cells with compounds **1–4** prevented the ROS production to 167.64, 164.36, 183.56, and 191.29 %, respectively. These observations suggest that compounds **1–4** could quench the oxidative stress induced by ROS in CCl_4-induced HepG2 cells.

Effect of compounds 1–4 on SOD activity in CCl_4-induced HepG2 cells

Mammalian cells are often equipped with a variety of antioxidative enzymes including catalase, GSH-Px, and SOD to protect against oxidative stress (Si et al. 2013). SOD catalyzes the dismutation of superoxide radical to H_2O_2 and this conversion is critical for alleviating oxidative stress (Flora 2009). One possible mechanism of hepatoprotective effects of compounds **1–4** might be related to the modulation of endogenous antioxidant enzymes. The effects of compounds **1–4** on intracellular SOD activity in CCl_4-induced HepG2 cells are shown in Fig. 4B; exposure of HepG2 cells to CCl_4 significantly decreased the activities of SOD to 36.57 % compared to that of control group. Pretreatment of cells with compounds **1–4** significantly attenuated the decrease of SOD to 77.65, 75.39, 76.58, and 62.58 %, respectively, compared to that of the control group.

Luciferase reporter gene assay and Western blot for measuring NF-κB transactivation

NF-κB, a heterodimer consisting of p65 and p50, is a major, well-documented transcription factor which is a

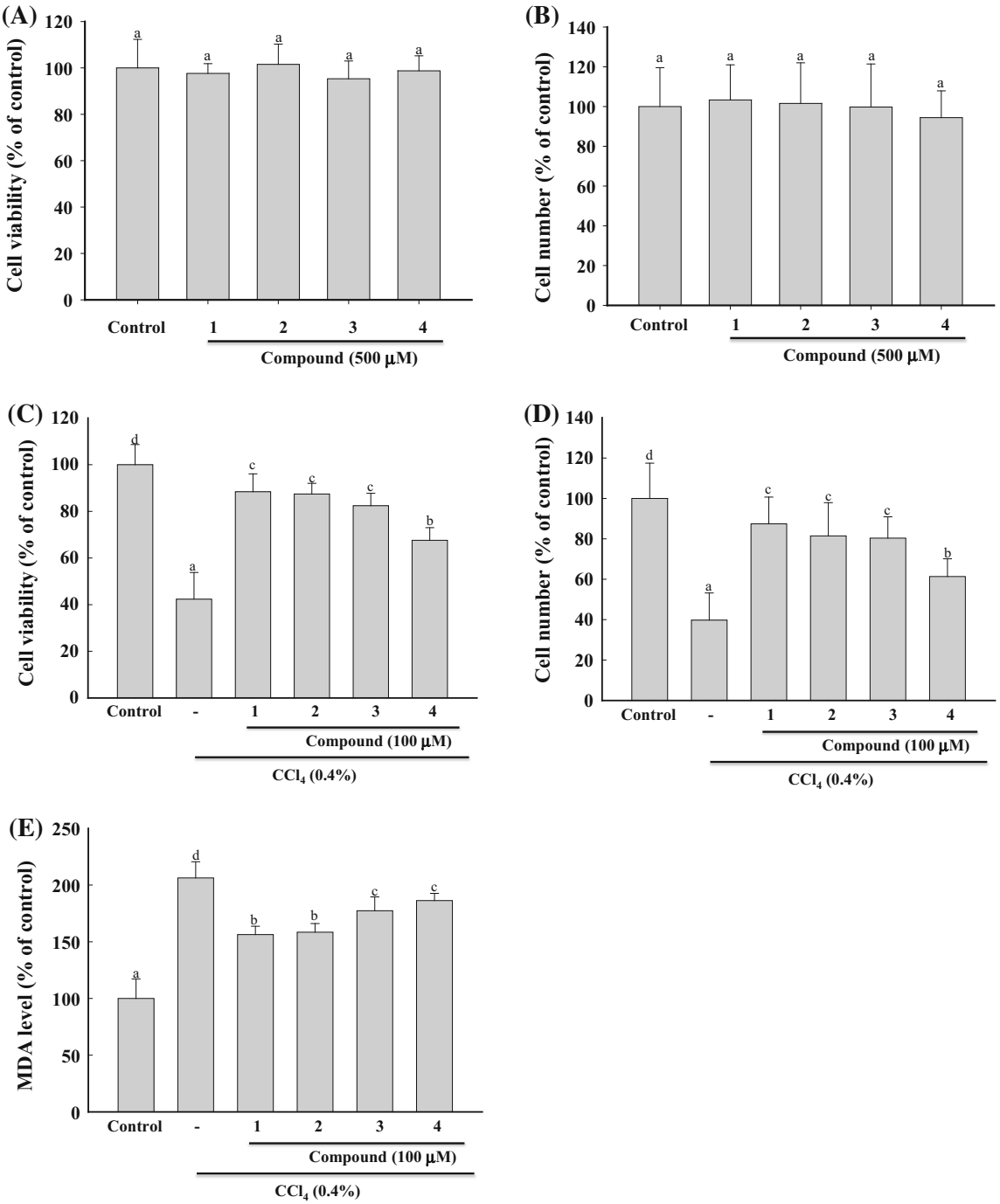

Fig. 3 Cytotoxicity and cytoproteoctive activity of compounds **1**–**4** obtained from *I. compacta*. HepG2 cells were incubated with different samples for 6 h by MTT (**A**) and trypan blue exclusion experiments (**B**). HepG2 cells were pretreated with different samples for 30 min before exposure to 0.4 % CCl_4 for 6 h. Then, cell viability was measured by the MTT (**C**) and trypan blue exclusion experiments (**D**). MDA content (**E**) in the cells were determined via spectrophotometry. The results were expressed as percentage of the control group. Data are presented as mean ± SD ($n = 3$). Values with the same superscript letters are not significantly different from each other at $p < 0.05$

master regulator of classical signaling pathway (Huxford and Ghosh 2009). Therefore, we examined whether the reduction of intracellular ROS production was associated with cell nuclear translocation of NF-κB using an NF-κB-luciferase reporter. As shown in Fig. 5A, cells were transfected with a luciferase reporter construct yielding a strong luciferase activity after stimulation by PMA, indicating that PMA activated NF-κB-mediated transcription

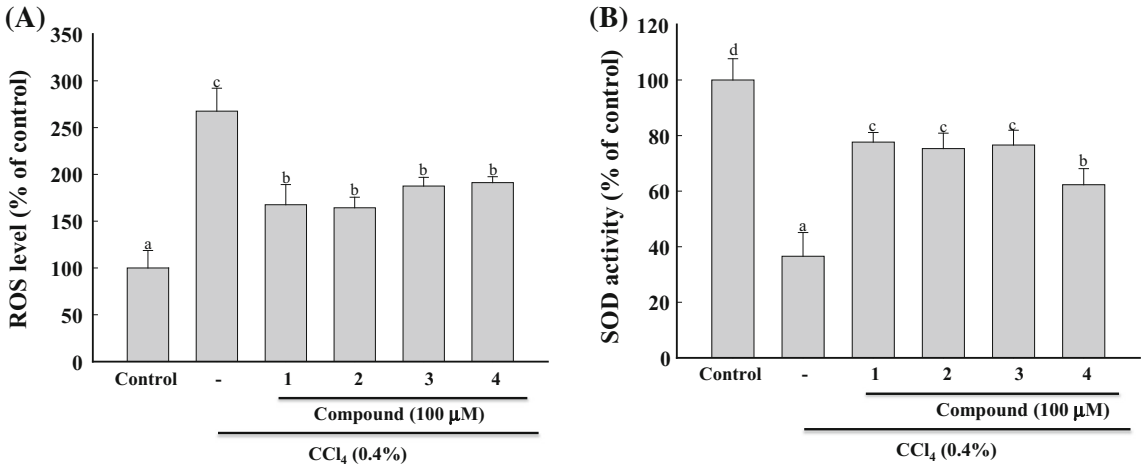

Fig. 4 Effect of compounds **1–4** obtained from *I. compacta* on CCl_4-induced intracellular ROS level and SOD activity. Intracellular ROS levels were measured using the DCFH-DA fluorescence. HepG2 cells were pretreated with different samples for 30 min before exposure to 0.4 % CCl_4 for 6 h. Histogram showing the ROS level (**A**) and SOD activity (**B**) in HepG2 cells after treatment with CCl_4 in the presence or absence of different samples compared to that of untreated groups. Values with the same superscript letters are not significantly different from each other at $p < 0.05$

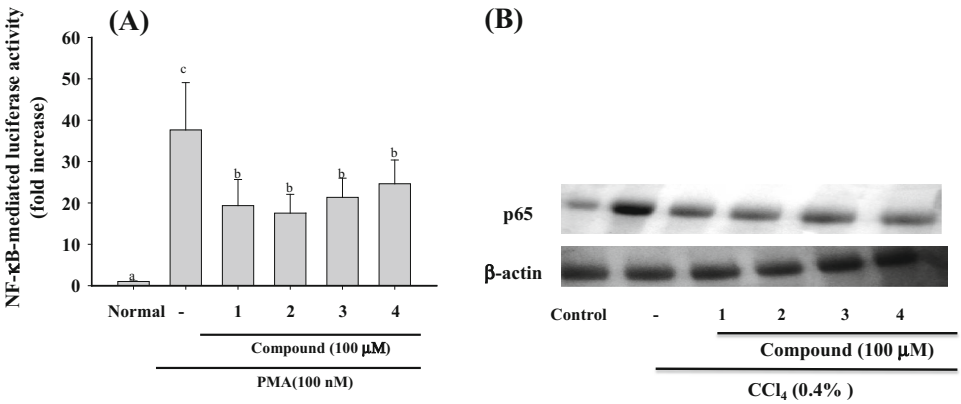

Fig. 5 Effect of compounds **1–4** obtained from *I. compacta* on NF-κB transactivation. HepG2 cells co-transfected with the plasmid constructs activating protein luciferase (NF-κB) (0.4 μg/mL) and β-gal (as a transfection control) were treated with different samples in the presence or absence of PMA for 24 h. Luciferase activity was determined by luminometry (**A**). After preparation of the nuclear fraction, the expression levels of p65 and β-actin were determined by Western blot (**B**). Values with the same superscript letters are not significantly different from each other at $p < 0.05$

in HepG2 cells, whereas the compounds **1–4** at 100 μM was found to abrogate activation of NF-κB to a higher degree. As shown in Fig. 5B, there is a sharp increase in the NF-κB p65 levels in the CCl_4-treated HepG2 cells; however, this NF-κB activation was inhibited by compounds **1–4**, implying that inhibition of NF-κB activation was tightly involved in the hepatoprotective effect of phenylethanoid glycosides.

In conclusion, this study was initiated to search for new active compounds from the roots of *I. compacta*. Four phenylethanoid glycosides were isolated through repeated column chromatography and preparative HPLC and identified on the basis of spectroscopic data analyses of NMR and MS. Compound **1–4** to some extent showed protective activity on CCl_4-induced cytotoxicity in HepG2 cells. Therefore, these results provide a probability for the biomedical use of phenylethanoid glycosides as hepatoprotectvie agents. Further studies are needed to determine the mechanisms of the isolated compounds.

Acknowledgments This work was financially supported from "Program for Innovative Research Team in IMPLAD", the technological large platform for comprehensive research and development of new drugs in the Twelfth Five-Year "Significant New Drugs Created" Science and Technology Major Projects (No. 2012ZX09301-002-001-026), Open Science Foundation of Jiangsu Key Laboratory for Biomass-based Energy and Enzyme Technology

(No. JSBEET1313), Natural Science Foundation of Jiangsu Province (No. BK20140455), and Natural Science Foundation of the Higher Education Institutions of Jiangsu Province (No. 14KJB550002 and 13KJB210001).

References

Adewusi EA, Afolayan AJ (2010) A review of natural products with hepatoprotective activity. J Med Plants Res 4:1318–1334

Afifi MS, Lahloub MF, El-Khayaat SA, Anklin CG, Rüegger H, Sticher O (1993) Crenatoside: a novel phenylpropanoid glycoside from *Orobanche crenata*. Planta Med 59:359–362

Akanitapichat P, Phraibung K, Nuchklang K, Prompitakkul S (2010) Antioxidant andhepatoprotective activities of five eggplant varieties. Food Chem Toxicol 48:3017–3021

Balasubramaniyan V, Shukla R, Murugaiyan G, Bhonde RR, Nalini N (2007) Mouse recombinant leptin protects human hepatoma HepG2 against apoptosis, TNF-α response and oxidative stress induced by the hepatotoxin-ethanol. Biochim Biophys Acta 1770:1136–1144

Barrera G (2012) Oxidative stress and lipid peroxidation products in cancer progression and therapy. ISRN Oncol 2012:137289

Bhardwaj A, Khatri P, Soni ML, Ali DJ (2011) Potent herbal hepatoprotective drugs-A review. J Adv Sci Res 2:15–20

Chattopadhyay RR (2003) Possible mechanism of hepatoprotective activity of *Azadirachta indica* leaf extract: part II. J Ethnopharmacol 89:217–219

Chi YM, Nakamura M, Zhao XY, Yoshizawa T, Yan WM, Hashimoto F, Kinjo J, Nohara T (2005) A monoterpene alkaloid from *Incarvillea sinensis*. Chem Pharm Bull 53:1178–1179

Dai N, Zou Y, Zhu L, Wang HF, Dai MG (2014) Antioxidant properties of proanthocyanidins attenuate carbon tetrachloride (CCl_4)-induced steatosis and liver injury in rats via CYP2E1 regulation. J Med Food 17:663–669

Delectis Florae Reipublicae Popularis Sinicae Agendae Academiae Sinicae Edita (1990) Flora Reipublicae Popularis Sinicae: Tomus 69. Science Press, Beijing, p 46

Flora SJ (2009) Structural, chemical and biological aspects of antioxidants for strategies against metal and metalloid exposure. Oxid Med Cell Longev 2:191–206

Fu JJ, Jin HZ, Shen YH, Zhang WD, Xu WZ, Zeng Q, Yan SK (2007) Two novel monoterpene alkaloid dimers from *Incarvillea arguta*. Helv Chim Acta 90:2151–2155

Fu GM, Pang HH, Wong YH (2008) Naturally occurring phenylethanoid glycosides: potential leads for new therapeutics. Curr Med Chem 15:2592–2613

Fu JJ, Qin JJ, Zeng Q, Huang Y, Jin HZ, Zhang WD (2010) Four new sesquiterpenoids from the roots of *Incarvillea arguta* against lipopolysaccharide-induced nitric oxide production. Chem Pharm Bull (Tokyo) 58:1263–1266

Gulçin I, Elmastas M, Aboul-Enein HYA (2012) Antioxidant activity of clove oil—a powerful antioxidant source. Arab J Chem 5:489–499

Hu WC, Wang G, Li P, Wang Y, Si CL, He J, Long W, Bai Y, Feng Z, Wang X (2014) Neuroprotective effects of macranthoin G from *Eucommia ulmoides* against hydrogen peroxide-induced apoptosis in PC12 cells via inhibiting NF-κB activation. Chem Biol Interact 224:108–116

Huxford T, Ghosh G (2009) A structural guide to proteins of the NF-κB signaling module. Cold Spring Harb Perspect Biol 1:a000075

Kashaw V, Nema AK, Agarwal A (2011) Hepatoprotective prospective of herbal drugs and their vesicular carriers–a review. Inter J Res Pharm Biomed Sci 2:361–374

Li CQ, Li BG, Qi HY, Li QL, Wang FP, Zhang GL (2004) Three cyclooctapeptides and one glycoside from *Microtoena prainiana*. J Nat Prod 67:978–982

Lobo V, Patil A, Phatak A, Chandra N (2010) Free radicals, antioxidants and functional foods: impact on human health. Pharmacogn Rev 4:118–126

Lu T, Zhang WD, Pei YH, Zhang C, Li JC, Shen YH (2007) A new iridoid from *Incarvillea delavayi*. Chin Chem Lett 18:1512–1514

Lu LH, Yang M, Lin S, Zheng Q, Zhang WD (2009) Chemical constituents from acetyl acetate extract fraction of *Incarvillea delavayi*. China J Chin Mater Med 34:1799–1801

Nakamura M, Chi YM, Yan WM, Nakasugi Y, Yoshizawa T, Irino N, Hashimoto F, Kinjo J, Nohara T, Sakurada S (1999) Strong antinociceptive effect of incarvillateine, a novel monoterpene alkaloid from *Incarvillea sinensis*. J Nat Prod 62:1293–1294

Nakamura M, Chi YM, Yan WM, Yonezawa A, Nakasugi Y, Yoshizawa T, Hashimoto F, Kinjo J, Nohara T, Sakurada S (2001) Structure-antinociceptive activity studies of incarvillateine, a monoterpene alkaloid from *Incarvillea sinensis*. Planta Med 67:114–117

Si CL, Shen T, Jiang YY, Wu L, Yu GJ, Ren XD, Xu GH, Hu WC (2013) Antioxidant properties and neuroprotective effects of isocampneoside II on hydrogen peroxide-induced oxidative injury in PC12 cells. Food Chem Toxicol 59:145–152

Yan YM, Wu GS, Dong XP, Shen L, Li Y, Su J, Luo HR, Zhu HJ, Cheng YX (2012) Sesquiterpenoids from *Incarvillea arguta*: absolute configuration and biological evaluation. J Nat Prod 75:1025–1029

Yang YC (1991) Handbook of tibetan medicine. Qinghai People's Press, Xining, p 465

Yang JY, Lee HS (2012) Evaluation of antioxidant and antibacterial activities of morin isolated from mulberry fruits (*Morus alba* L.). J Korean Soc Appl Biol Chem 55:485–489

Yang JH, Hu JP, Rena K, Du NS (2009) Structure-activity relationships of phenylethanoid glycosides in plants of *Cistanche salsa* on antioxidative activity. Zhong Yao Cai 32:1067–1069

Yu WG, Qian J, Lu YH (2011) Hepatoprotective effects of 2′,4′-dihydroxy-6′-methoxy-3′,5′-dimethylchalcone on CCl_4-induced acute liver injury in mice. J Agric Food Chem 59:12821–12829